Electronic Supplementary Material (ESI) for Sustainable Energy & Fuels.

Electronic Supplementary Information

A1. Gas behavior using constrained equilibrium thermodynamic approach

Figures A1.1 to A1.5 show comparison results for the main gaseous products predicted by unconstrained (FACTSAGE^{TM} simulation) and constrained models and experimental data for all the three different biomass wastes. Comparison study for each biomass type has been conducted at specific temperatures and pressures. The analysis includes case studies for each biomass Case A involves no additional constraints and gas compositions are based on the GTE approach. Case B uses carbon gasification efficiency as the only additional constraint. Case C uses carbon gasification efficiency along with a specific amount of CH_4 obtained from experiments as additional constraints. Case D employs carbon gasification efficiency together with specific amounts of CH_4 and H_2 obtained from experiments as additional constraints. It is worth noting that carbon gasification efficiencies have been determined using experimental data. The overall view of the data used for constrained equilibrium analysis is listed in Table A1.1.

Table A1.1: Additional constraint values used for modeling.

Biomass feed	Experimental conditions (T (°C) / P (bar))	Carbon gasification efficiency (%)	CH_4 amount (mol/kg$_{biomass}$ on d.b.)	H_2 amount (mol/kg$_{biomass}$ on d.b.)
Manure	539 / 270	72.0	7.9	4.9
Fruit/vegetable waste	545 / 230	73.0	6.8	6.9
Fruit/vegetable waste	483 / 235	64.0	5.4	5.5
Cheese whey	543 / 230	82.8	7.2	7.3
Cheese whey	498 / 240	53.2	3.6	6.9

As evident in Figures A1.1 to A1.5, Case A which shows the results of GTE approach does not hold a satisfactory agreement with gas compositions obtained from experiments. Similarly, Cases B and C do not show good agreement with the experimental product gas compositions. However, Case D, where three additional constraints are used reveals good agreement with experimental data. The results of Case D demonstrate that integration of CGE value and experimental values of CH_4 and H_2 into the model shall result in better accuracy.

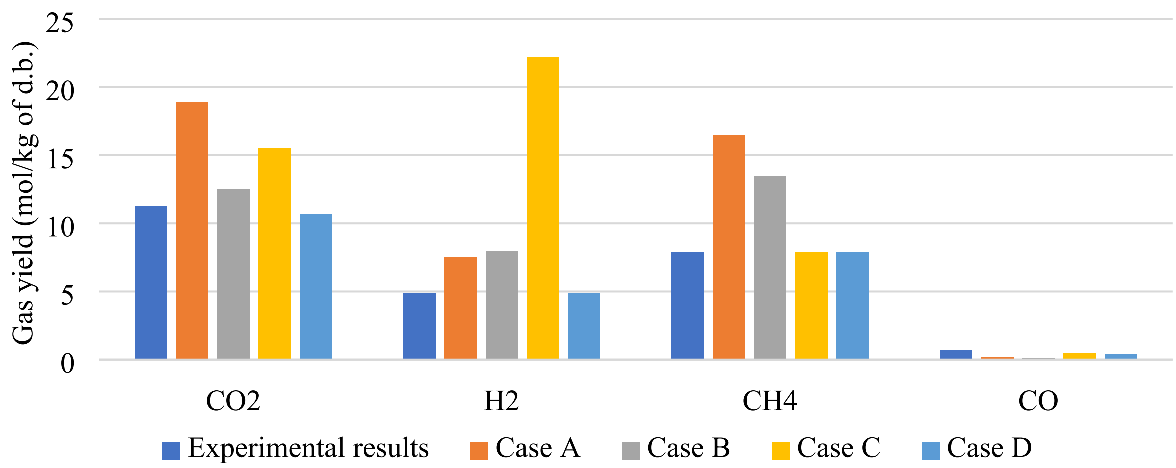

Figure A1.1: Comparison between different modeling approaches and experimental values for manure at 539 °C and 270 bar with a feed concentration of 17 wt%. Case A includes only GTE values, Case B includes CGE as constraint, Case C includes CGE + constant amount of CH_4 as constraints, Case D includes CGE + constant amount of CH_4 and H_2 as constraints.

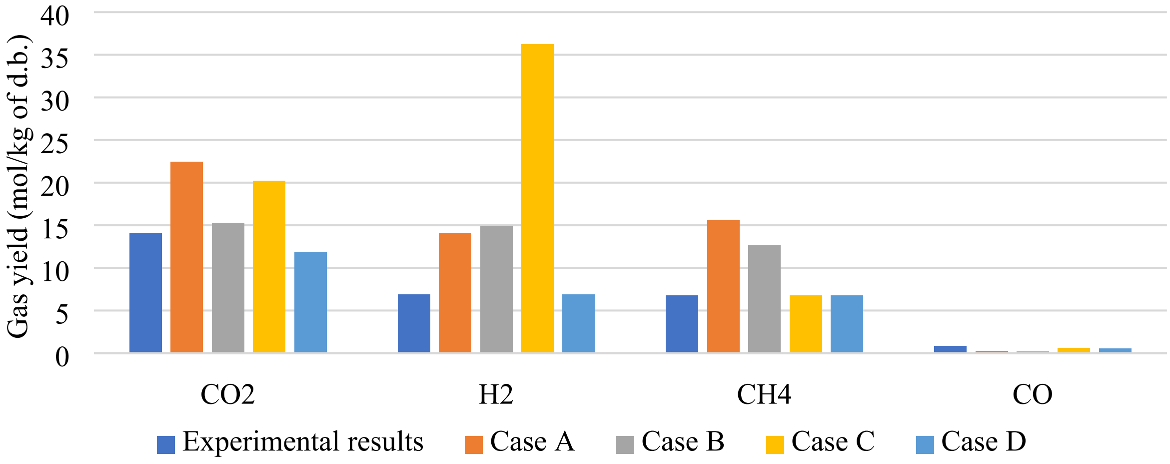

Figure A1.2: Comparison between different modeling approaches and experimental values for fruit/vegetable waste at 545 °C and 230 bar with a feed concentration of 11 wt%. Case A includes only GTE values, Case B includes CGE as constraint, Case C includes CGE + constant amount of CH_4 as constraints, Case D includes CGE + constant amount of CH_4 and H_2 as constraints.

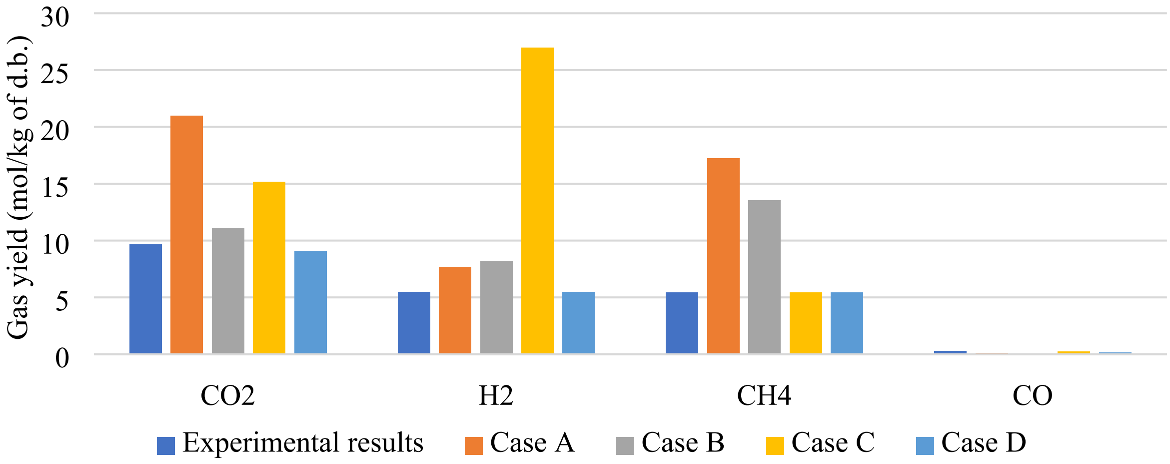

Figure A1.3: Comparison between different modeling approaches and experimental values for fruit/vegetable waste at 483 °C and 235 bar with a feed concentration of 11 wt%. Case A includes only GTE values, Case B includes CGE as constraint, Case C includes CGE + constant amount of CH_4 as constraints, Case D includes CGE + constant amount of CH_4 and H_2 as constraints.

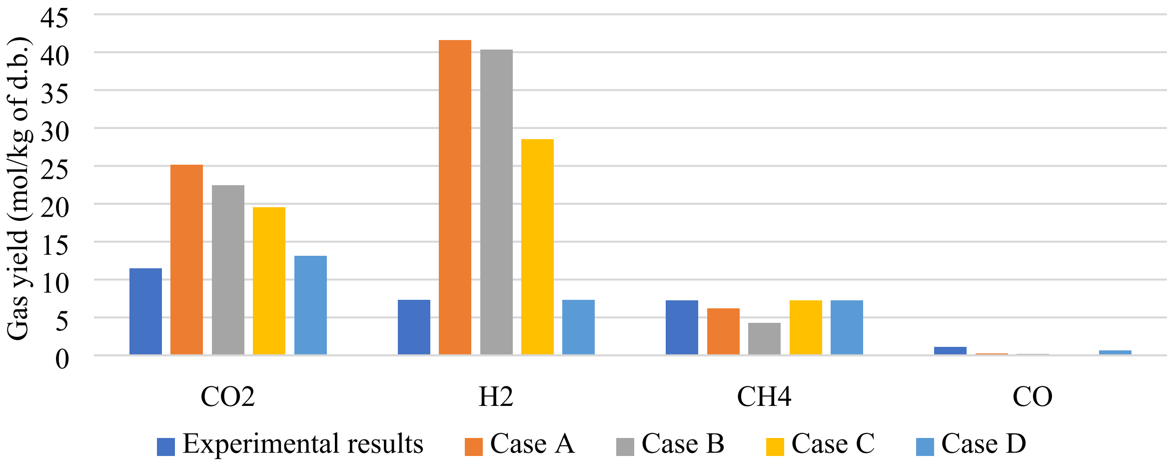

Figure A1.4: Comparison between different modeling approaches and experimental values for cheese whey at 543 °C and 230 bar with a feed concentration of 3 wt%. Case A includes only GTE values, Case B includes CGE as constraint, Case C includes CGE + constant amount of CH_4 as constraints, Case D includes CGE + constant amount of CH_4 and H_2 as constraints.

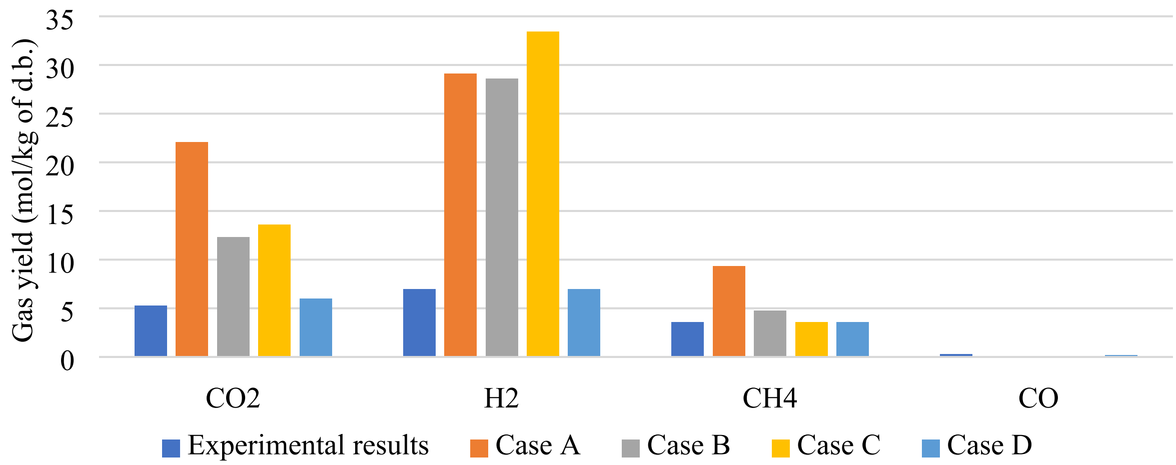

Figure A1.5: Comparison between different modeling approaches and experimental values for cheese whey at 498 °C and 240 bar with a feed concentration of 3 wt%. Case A includes only GTE values, Case B includes CGE as constraint, Case C includes CGE + constant amount of CH4 as constraints, Case D includes CGE + constant amount of CH4 and H2 as constraints.

B1. Elemental partitioning behavior of manure

Figure B1.1 (a-e) shows the elemental partitioning behavior for manure. Results are based on SCWG for fruit/vegetable waste at 240 bar and a temperature range of 100-700 °C. For this purpose, FACTSAGE^{TM} simulations are performed under subcritical conditions for a temperature range of 100-375 °C whilst 400-700 °C temperature range considered for supercritical conditions.

Figure B1.1 (a) exhibits the partitioning behavior of potassium. The results show that KOH, in its dissolved aqueous form, is mainly formed along with small quantities of K+ ions in the subcritical region. The supercritical region only consists of solid compounds of potassium in the form of $K_2Ca_2(CO_3)_3$ mainly present at temperatures below 525 °C and $K_2Ca(CO_3)_2$ dominating beyond 550 °C along with smaller quantities of K_2CO_3.

Figure B1.1 (b) illustrates the partitioning behavior of calcium. The results reveal that calcium is only present in solid compound forms within the entire temperature range of 100-700 °C. Moreover, $CaCO_3$ is mainly present in the subcritical region along with smaller quantities of $Na_2CaP_2O_7$. In the supercritical region between 400-525 °C, $K_2Ca2(CO_3)_3$ is mainly present while $K_2Ca(CO_3)_2$ appears in small quantities at temperatures higher than 550 °C. Furthermore, $Ca_5(OH)(PO_4)_3$ is present in the entire considered temperature range. However, it is mainly formed in the supercritical region at temperatures exceeding 550 °C.

The partitioning behavior of magnesium is shown in Figure B1.1 (c). The figure shows that the only stable form of magnesium is Mg(butanoate)$_2$ in the subcritical region, wherein it is presented in its dissolved aqueous form. Only solid forms of magnesium compounds are present in the supercritical region with the compound form of $NaMgPO_4$, MgO, $Mg_5Al_2Si_3O_{10}(OH)_8$, $KMg_3AlSi_3O_{10}(OH)_2$, Mg_2SiO_4, and $MgCO_3$. Furthermore, $MgCO_3$ and MgO are mainly present in the temperature range of 400-500 °C and at temperatures higher than 550 °C, respectively.

The partitioning behavior of sodium is shown in Figure B1.1 (d). The results demonstrate that at temperatures lower than 375 °C, four compounds of sodium are present including solid $Na_2CaP_2O_7$, Na^+ ion, solid $NaAlSiO_4$, and aqueous $NaHCO_3$. The subcritical region is dominated by solid $Na_2CaP_2O_7$ with an average mole fraction of 64%. Between 400-525 °C and at temperatures exceeding 550 °C, the most stable forms present are $NaMgPO_4$, and Na_2CO_3, in their solid forms. Solid $Na_2Ca_3Al_{16}O_{28}$ is present in very small quantities in the supercritical range.

As shown in Figure B1.1 (e), only solid forms of iron compounds are present in the entire evaluated temperature range. At temperatures below 200 °C, the only stable compound present is FeS2. In between 225 °C and 375 °C, FeS2, FeS (s2), Fe_3O_4, and FeS (s3) are present in different quantities. In the higher temperature supercritical region, the only stable form of iron is Fe_2O_3.


(a)
Partioning behavior of potassium
Mole fraction (%)
Temperature (°C)
K^+ (aq) KOH (aq) $KHCO_2$ (aq) K_2CO_3 (s) $K_2Ca2(CO_3)_3$ (s) $K_2Ca(CO_3)_2$ (s)
(b)
Partioning behavior of calcium
Mole fraction (%)
Temperature (°C)
$Ca_5HO_{13}P_3$ (s) $Na_2Ca_3Al_{16}O_{28}$ (s) $Na_2CaP_2O_7$ (s) $K_2Ca(CO_3)_2$ (s) CaCO3 (s2) $K_2Ca2(CO_3)_3$ (s)
(c)
Partioning behavior of magnesium
Mole fraction (%)
Temperature (°C)
$Mg(butanoate)_2$ (aq) $NaMgPO_4$ (s) MgO (s) $Mg_5Al_2Si_3O_{10}(OH)_8$ (s) $KMg_3AlSi_3O_{10}(OH)_2$ (s) Mg_2SiO_4 (s) $MgCO_3$ (s)
(d)
Partioning behavior of sodium
Mole fraction (%)
Temperature (°C)
$Na_2CaP_2O_7$ (s) Na^+ (aq) Na_2CO_3 (s) $NaMgPO_4$ (s) $NaAlSiO_4$ (s) $NaHCO_2$ (aq) $Na_2Ca_3Al_{16}O_{28}$ (s)

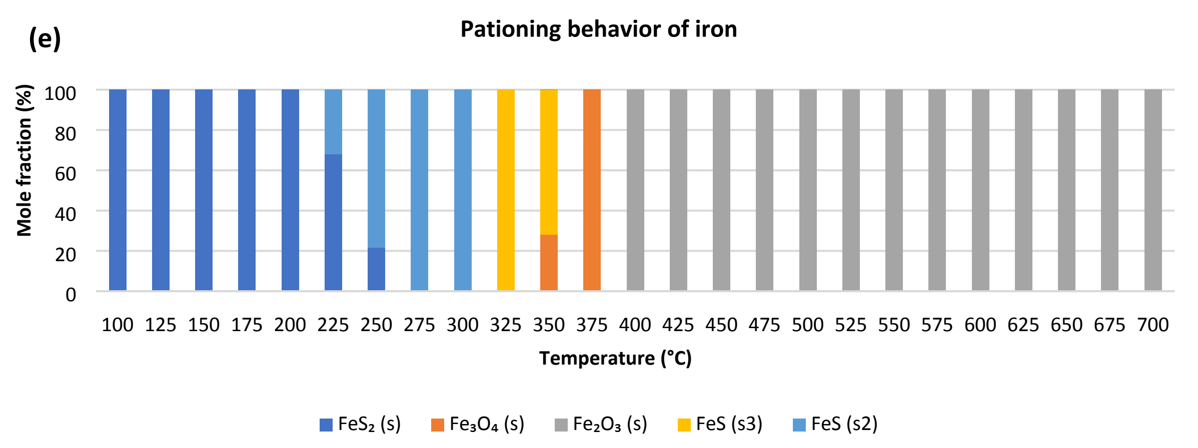

Figure B1.1: Partitioning behavior of: (a) potassium, (b) calcium, (c) magnesium, (d) sodium, (e) iron compounds during supercritical water gasification of manure for a temperature range of 100-700 °C at 24 MPa having a concentration of 17 wt%.

B2. Elemental partitioning behavior of fruit/vegetable waste

Figure B2.1 (a-h) shows the elemental partitioning behavior for fruit/vegetable waste. Results are based on SCWG for fruit/vegetable waste at 240 bar and a temperature range of 100-700 °C. For this purpose, FACTSAGE^{TM} simulations are performed under subcritical conditions for a temperature range of 100-375 °C whilst 400-700 °C temperature range considered for supercritical conditions.

As shown in Figure B2.1 (a), the first region which lies between 100-325 °C is dominated by solid carbon in the form of graphite along with small amounts of Mg (butanoate)$_2$ and $CaCO_3$. While the second region in the range of 350 – 700 °C shows the dominance of gas products such as CO2, CH4, and CO followed by the appearance of other compounds such as $K_2Ca_2(CO3)_3$, K_2CO_3, and HCO_3^- present in smaller quantities. The trend can be explained as above 350 °C solid carbon decomposes to form CO_2 and CH_4. CH_4 further starts decomposing around 400 °C and gets converted into CO_2, CO and H_2.

Partitioning behavior of sulfur is shown in Figure B2.1 (b). Around 100 °C, an approximate of 20% molar fraction of K2SO4 in the solid form gets formed. Between 100-325 °C, the region is mainly dominated by KSO_4^- and HS- followed by SO_4^{2-}, aqueous H_2S, and ZNS (s) present in smaller quantities. KSO_4^- decreases with an increase in temperature while HS- increases. The region between 375 °C and 700 °C is dominated by the gaseous form of H_2S.

As shown in Figure B2.1 (c), phosphorous compounds are only present in solid form in the entire gasification temperature range, phosphorus compounds are only present in solid form. At temperatures lower than 375 °C, phosphorus is present mainly in two forms, $Ca_5(OH)(PO_4)_3$ and $Na_2CaP_2O_7$ with an average of 70% and 20%, respectively. The region also contains smaller quantities of $HP_2O_7^{3-}$ HPO_4^{2-}, $P_2O_7^{2-}$, and $H_2PO_4^-$. Between 400 °C and 450 °C, the region is dominated by $Mg_3P_2O_8$ with an average of 50% molar fraction, while $NaMgPO_4$ and $Ca_5(OH)(PO_4)_3$ present in small quantities (average of 25% each). At temperatures exceeding 475°C is dominated by $Ca_5(OH)(PO_4)_3$.

Partitioning behavior of nitrogen is shown in Figure B2.1 (d). At temperatures lower than 325 °C, the region is dominated by N_2 in its aqueous form while containing smaller quantities of N_2 in its gaseous form and NH_3 in its aqueous form. Nitrogen in the form of N_2 gas is the most stable compound present between 350 °C and 400 °C along with smaller quantities of NH3(g). At temperatures higher than 400 °C, the only stable compound present is NH_3(g).

Partitioning behavior of potassium is shown in Figure B2.1 (e). In the subcritical region, KOH in its dissolved aqueous form and K+ ions are mainly formed, with K+ ions decreases with increase in temperature while KOH (aq) increases. The supercritical region only consists of solid compounds of potassium in the form of $K_2Ca2(CO_3)_3$ present at temperatures lower than 450 °C along with K_2CO_3. At temperatures exceeding 450 °C, K_2CO_3 is the only stable compound present.

Partitioning behavior of calcium is shown in Figure B2.1 (f). Analysis suggests that calcium is only present in its solid form in the entire temperature range of 100-700 °C. $Ca_5(OH)(PO_4)_3$ is mainly present in the subcritical region along with smaller quantities of $Na_2CaP_2O_7$. In the supercritical region between 400-450 °C, $Ca_5(OH)(PO_4)_3$ along with $K_2Ca(CO_3)_2$ and $CaCO_3$ are present. Furthermore, at temperatures higher than 475 °C, the region is dominated by $Ca_5(OH)(PO_4)_3$ along with small quantities of $CaCO_3$.

Partitioning behavior of magnesium is shown in Figure B2.1 (g). In the subcritical region, the only stable form of magnesium is Mg (butanoate)$_2$, wherein it is present in its aqueous form. Only solid forms of magnesium compounds are present in the supercritical region including $NaMgPO_4$, MgO, $Mg_3P_2O_8$, $Mg_3B_2O_6$, and Mg $(OH)_2$. Mg $(OH)_2$ can be found only between 475 °C and 500 °C.

Partitioning behavior of sodium is shown in Figure B2.1 (h). Results suggest that at temperatures below 375 °C, $Na_2CaP_2O_7$ is the most stable form present with Na+ ions found only at around 375 °C. At temperatures exceeding 400 °C, the region is dominated by $NaMgPO_4$ with small quantities (average of 35% molar fraction) of Na_2CO_3 present between 600 °C and 700 °C.

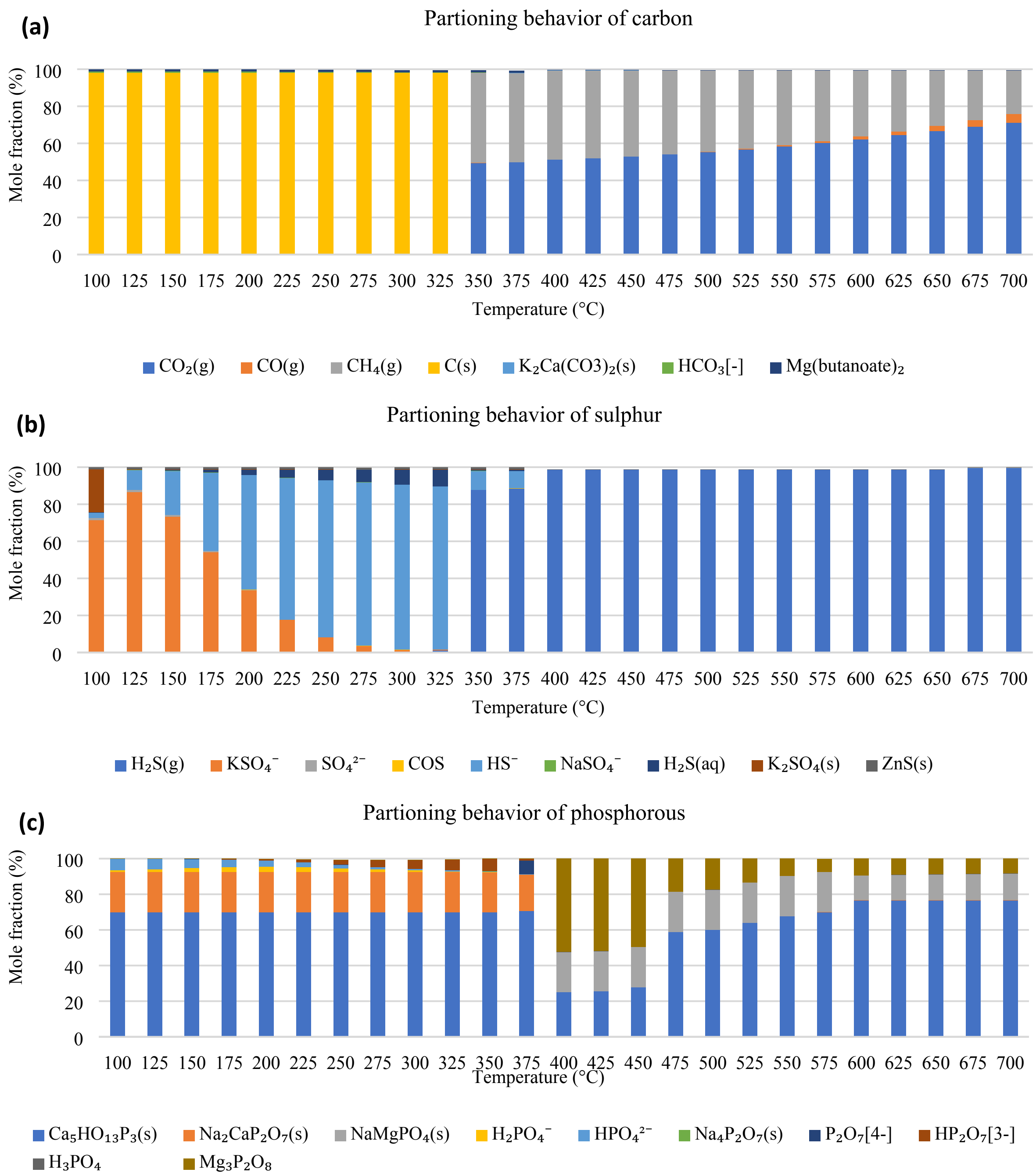

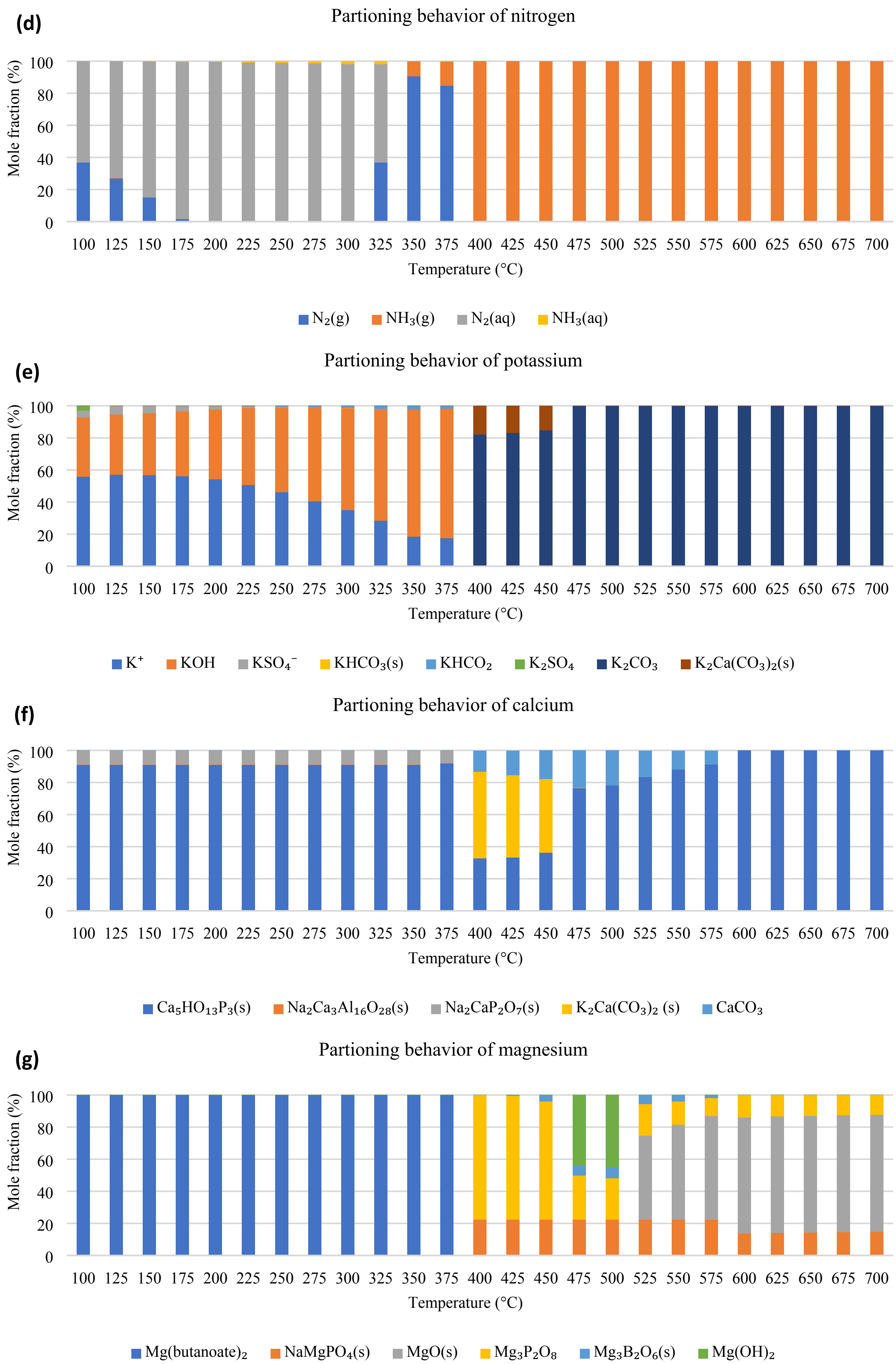
(d)
Partioning behavior of nitrogen
Mole fraction (%)
0 20 40 60 80 100
100 125 150 175 200 225 250 275 300 325 350 375 400 425 450 475 500 525 550 575 600 625 650 675 700
Temperature (°C)
N₂(g) NH₃(g) N₂(aq) NH₃(aq)
(e)
Partioning behavior of potassium
Mole fraction (%)
0 20 40 60 80 100
100 125 150 175 200 225 250 275 300 325 350 375 400 425 450 475 500 525 550 575 600 625 650 675 700
Temperature (°C)
K⁺ KOH KSO₄⁻ KHCO₃(s) KHCO₂ K₂SO₄ K₂CO₃ K₂Ca(CO₃)₂(s)
(f)
Partioning behavior of calcium
Mole fraction (%)
0 20 40 60 80 100
100 125 150 175 200 225 250 275 300 325 350 375 400 425 450 475 500 525 550 575 600 625 650 675 700
Temperature (°C)
Ca₅HO₁₃P₃(s) Na₂Ca₃Al₁₆O₂₈(s) Na₂CaP₂O₇(s) K₂Ca(CO₃)₂ (s) CaCO₃
(g)
Partioning behavior of magnesium
Mole fraction (%)
0 20 40 60 80 100
100 125 150 175 200 225 250 275 300 325 350 375 400 425 450 475 500 525 550 575 600 625 650 675 700
Temperature (°C)
Mg(butanoate)₂ NaMgPO₄(s) MgO(s) Mg₃P₂O₈ Mg₃B₂O₆(s) Mg(OH)₂

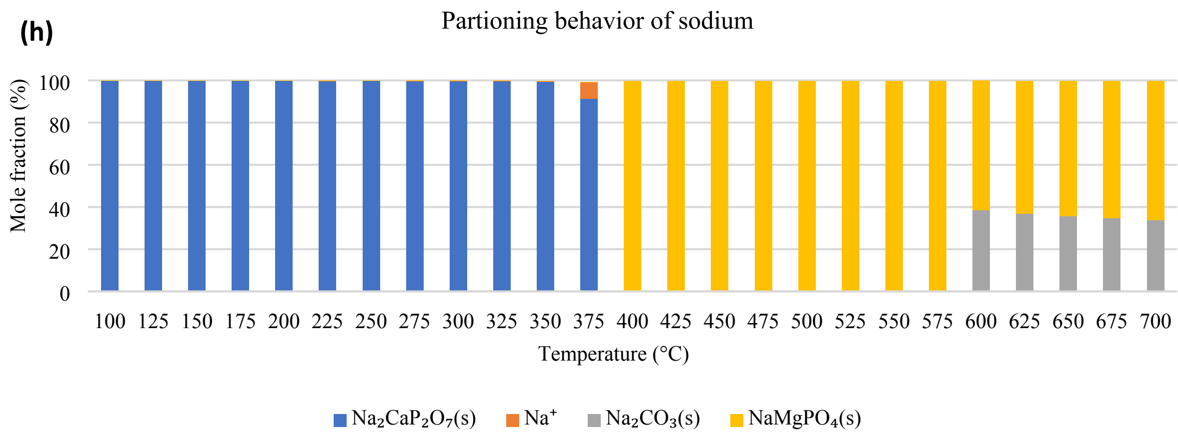

Figure B2.1: Partitioning behavior of: (a) carbon, (b) sulfur, (c) phosphorous, (d) nitrogen, (e) potassium, (f) calcium, (g) magnesium, and (h) sodium during supercritical water gasification of fruit/vegetable waste for a temperature range of 100-700 °C at 24 MPa having a concentration of 11 wt%.

B3. Elemental partitioning behavior of cheese whey

Figures B3.1 (a-g) show the elemental partitioning behavior results for cheese whey. Results are based on the SCWG for fruit/vegetable waste at 240 bar and a temperature range of 100-700 °C. For this, FACTSAGE^{TM} simulations are under subcritical conditions for a temperature range of 100-375 °C, while 400-700 °C considered under supercritical conditions.

As shown in Figure B3.1 (a), the first region which lies between 100-325 °C is dominated by solid carbon in the form of graphite along with small amounts of Mg (butanoate)$_2$ and $CaCO_3$(s2) and CH_4(aq). While the second region, lying beyond 350 °C, shows the dominance of gas products such as CO_2, CH_4, and CO followed by appearances of other compounds like K_2CaCO_3 (s2), K_2CO_3, and HCO_3^- present in smaller quantities. The trend can be explained as at temperatures higher than 350 °C solid carbon decomposes to form CO_2 and CH_4. CH_4 further starts decomposing around 400 °C and gets converted into CO_2, CO and H_2.

Partitioning behavior of sulfur is shown in Figure B3.1 (b). Between 100-325 °C, the region is mainly HS- followed by aqueous H_2S and ZNS(s) present in smaller quantities. At temperatures exceeding 350 °C, H_2S is the most stable form with smaller quantities of ZNS present in its solid form.

Partitioning behavior of phosphorous is shown in Figure B3.1 (c) which suggests that phosphorus compounds are only present in their solid forms in the entire gasification temperature range. At temperatures below 400 °C, phosphorus is present mainly in the form of $Na_2CaP_2O_7$, while $Ca_5(OH)(PO_4)_3$ and $NaMgPO_4$ present in small quantities. At temperatures higher than 400 °C mainly consists of $Ca_5(OH)(PO_4)_3$ with small quantities of $NaMgPO_4$ and Na_3PO_4.

Partitioning behavior of potassium is shown in B3.1 (d). KOH in its dissolved aqueous form is mainly formed with small quantities of K+ ions and $KHCO_2$ present in the subcritical region at temperatures lower than 375 °C. Around 400 °C, $K_2Ca2(CO_3)_2$ gets formed with a molar fraction of 95%. Between 425 °C and 700 °C, K_2CO_3 is the most stable compound present with small quantities of $K_2Ca2(CO_3)_2$ at temperatures below 500 °C.

Partitioning behavior of calcium is shown in Figure B3.1 (e). Results depict that calcium compounds are only present in their solid forms in the entire gasification temperature range of 100-700 °C. The subcritical region consists of three calcium compounds $Ca_5(OH)(PO_4)_3$, $CaCO_3$(s2), and $Na_2CaP_2O_7$. Around 400 °C, $K_2Ca2(CO_3)_2$ appears with a molar fraction of 70% along with $Na_2CaP_2O_7$ and $Ca_5(OH)(PO_4)_3$. Between 425 °C and 700 °C, $Ca_5(OH)(PO_4)_3$ gets mainly formed with smaller quantities of $K_2Ca2(CO_3)_2$ present at temperatures lower than 500°C.

Partitioning behavior of magnesium is shown in Figure B3.1 (f). Results show that the only stable form of magnesium is Mg (butanoate)$_2$ in the subcritical region at temperatures below 375 °C, wherein it is present in its aqueous form. Only solid forms of magnesium compounds are present in the supercritical region with $NaMgPO_4$ decreasing while MgO increasing in the supercritical temperature range.

Partitioning behavior of sodium is shown in Figure B3.1 (g). The displayed results show that at temperatures lower than 400 °C, $Na_2CaP_2O_7$ is the most stable form present with Na+ ions found in small quantities and $NaMgPO_4$(s) appears at 400 °C. Between 400 °C and 600 °C, the region is dominated by Na_2CO_3(s) along with small quantities of $NaMgPO_4$(s). At temperatures exceeding 600 °C, Na_2CO_3(s) starts decreasing while Na_3PO_4(s) starts increasing.


(a)
Partioning behavior of carbon
Mole fraction (%
Temperature (°C)
CO2(g)
CO(g)
CH4(g)
C(s)
K2Ca(CO3)2(s)
HCO3[-]
Mg(butanoate)2
K2CO3
CaCo3(s2)
Na2CO3
CO3[2-]
n-octylbenzene
CH4(aq)
(b)
Paritoning behavior of sulphur
Mole fraction (%)
Temperature (°C)
H2S(g)
ZnS(s)
H2S(aq)
HS[-]
(c)
Partioning behavior of phosphorous
Mole fraction (%)
Temperature (°C)
Ca5HO13P3(s)
Na2CaP2O7(s)
NaMgPO4(s)
Na3PO4
(d)
Partioning behavior of potassium
Mole fraction (%)
Temperature (°C)
K+
KOH(aq)
KHCO2
K2CO3
K2Ca(CO3)2(s)

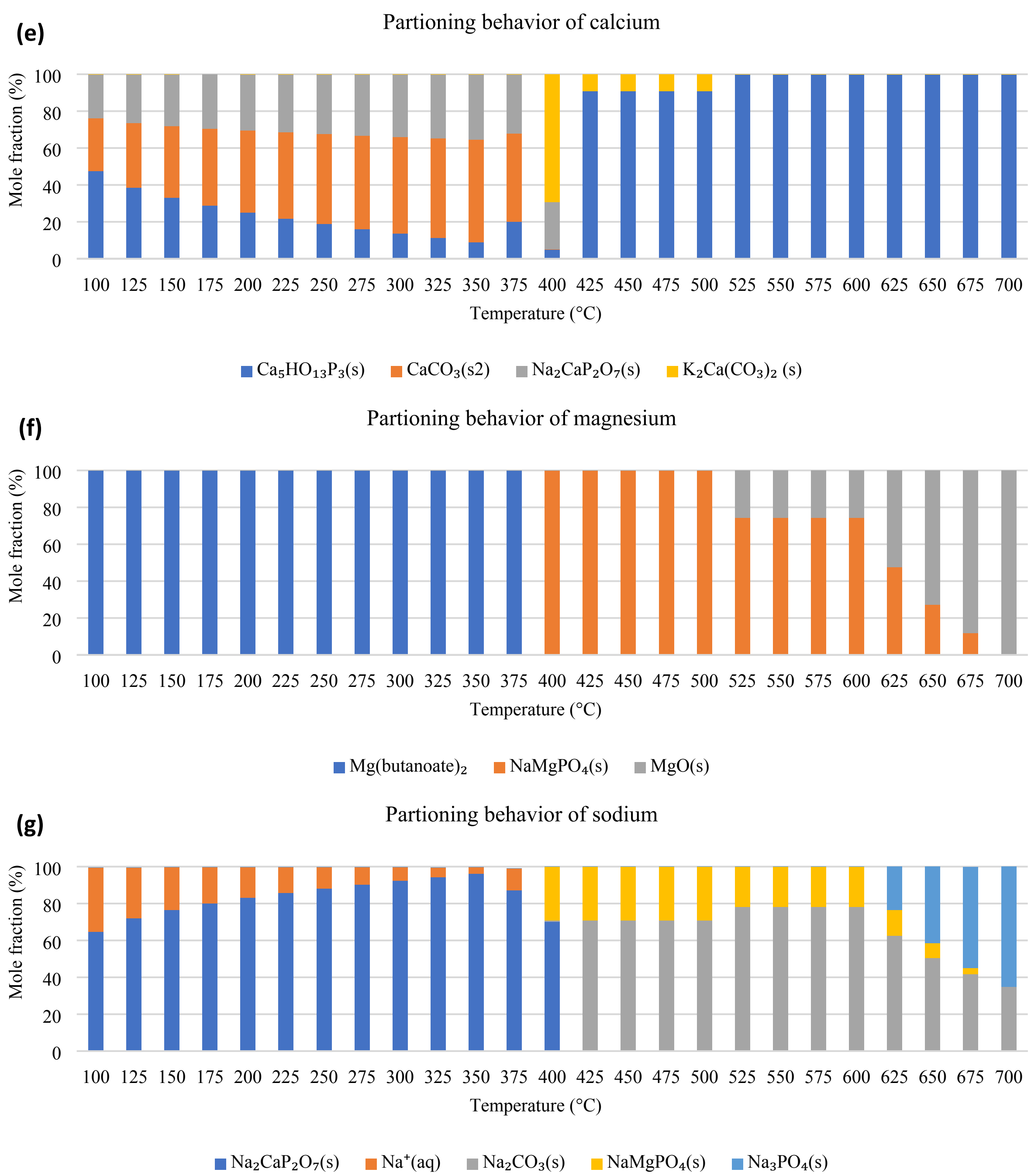

Figure B3.1: Partitioning behavior of: (a) carbon, (b) sulfur, (c) phosphorous, (d) potassium, (e) calcium, (f) magnesium, and (g) sodium during supercritical water gasification of fruit/vegetable waste for a temperature range of 100-700 °C at 24 MPa having a concentration of 3 wt%.